## A Data-Driven Modeling and Control Framework for Physics-Based Building Emulators

Chihyeon Song \* Aayushman Sharma \* Raman Goyal Alejandro Brito Saman Mostafavi \*

\* Palo Alto Research Center, Inc. (PARC), Palo Alto, CA 94304 USA (e-mail: {csong, asharma, raoyal, abrito, smostafa}@parc.com).

Abstract: We present a data-driven modeling and control framework for physics-based building emulators. Our approach comprises: (a) Offline training of differentiable surrogate models that speed up model evaluations, provide cheap gradients, and have good predictive accuracy for the receding horizon in Model Predictive Control (MPC) and (b) Formulating and solving nonlinear building HVAC MPC problems. We extensively verify the modeling and control performance using multiple surrogate models and optimization frameworks for different available test cases in the Building Optimization Testing Framework (BOPTEST). The framework is compatible with other modeling techniques and customizable with different control formulations. The modularity makes the approach future-proof for test cases currently in development for physics-based building emulators and provides a path toward prototyping predictive controllers in large buildings.

Keywords: Data-driven control, Nonlinear model predictive control, Building emulator, Surrogate modeling.

#### 1. INTRODUCTION

According to recent estimates by United States Energy Information Administration (2021), residential and commercial buildings account for nearly 40\% of energy usage in the United States. A significant amount of this energy consumption can be eliminated by improving the building's HVAC control system, for example using predictive control methods as has been shown in Drgoňa et al. (2020). Among these methods, model predictive control (MPC) is a particularly powerful approach for handling constraints for state and control inputs in nonlinear multivariable control systems. While the gains are evident, the challenge is to show that MPC can be implemented at scale in a cost-friendly manner (O'Dwyer et al., 2022). It is well understood that the main obstacle to this is the modeling cost and according to one study (Atam and Helsen, 2016), this can be as much as 70% of the total effort of setting up an MPC-based building controller, mainly due to the effort and expertise required to create realistically calibrated models. Recently, Building Optimization Testing Framework (BOPTEST) (Blum et al., 2021) is developed to facilitate simulation-based benchmarking of building HVAC control algorithms. The emulator uses calibrated Modelica models to emulate building physical dynamics based on first principles. Models also output Key Performance Indices (KPI) that represent occupant satisfaction, energy cost and consumption, and carbon footprint. What makes this platform even more impressive is the fact that it is set up to replicate a real building control system with

all its control limitations, e.g., there are realistic low-level feedback control laws, box constraints on control inputs, weather, occupancy profiles, economizer schedules, etc.

MOTIVATION While the value of BOPTEST, and other physics-based emulators in creating a unified testing platform for control is unquestionable, there are several intrinsic obstacles to the implementation of predictive control and its adoption by a broader audience 1: (1) In BOPTEST, and most other physic-based emulators, the numerical solvers for scaled-up models will not be computationally efficient to run in iterative optimization loops. (2) Solving the optimization problem requires gradient calculations which, derived through perturbations, only compounds the computational intensity. (3) Furthermore, some optimal control methods, such as iterative Linear Quadratic Regulator method (iLQR) (Todorov and Li, 2005), derive optimal solutions by exploring trajectories that might be infeasible for the emulator to evaluate (due to control input and state constraints), which can lead to crashing the iterative algorithm prematurely.

While acknowledging the significant progress in deep neural networks-based reinforcement learning (RL) approaches for controlling unknown dynamical systems, with applications expanding from playing games (Silver et al., 2016), locomotion (Lillicrap et al., 2015) and robotic hand manipulation (Levine et al., 2016), RL is still highly data intensive. The training time for such algorithms is typically

<sup>\*</sup> Chihyeon Song and Aayushman Sharma contributed equally to this paper. Saman Mostafavi is the corresponding author.

<sup>&</sup>lt;sup>1</sup> It is worth mentioning that we consider these challenges to be almost identical for a real building HVAC control system and, therefore, addressing and solving them is a first step to deploying such control algorithms in the field.

very large, and high variance and reproducibility issues mar the performance Henderson et al. (2018). At the moment, RL algorithms remain intractable for adjustable and reproducible implementations at scale. On the other hand, most of the building MPC work (Sturzenegger et al., 2015; Mostafavi et al., 2022; Oei et al., 2020; Walker et al., 2017) consider either simple low-fidelity RC-based models, bilinear models with low accuracy, Machine Learning (ML) approaches that cannot be directly used for fast MPC implementation, or directly use Modelica-based models with hand-tuned cost functions for nonlinear optimization of energy consumption. Such modeling and control approaches require a lot of customization for high-fidelity models with complex, hybrid, and constrained systems that use external inputs and therefore, are not suited to a robust control framework.

CONTRIBUTIONS The main contribution of this paper is the development of a modeling and control framework for building HVAC control based on identifying differentiable models that are compatible with optimization-based nonlinear optimal control methods. We address these limitations by the following two-fold approach: first, in an off-line round, we identify a differentiable surrogate model for the following nonlinear mapping:

$$x_{t+1} = f(x_t, u_t, d_t) \tag{1}$$

where x represent the state of the model, u the control inputs, and d the external time-varying disturbances, associated with the weather and occupancy conditions. Second, we use automatic differentiation (AD) (Paszke et al., 2017) to compute gradients for solving nonlinear model predictive control (NMPC) with box constraints for state and inputs. The details for modeling and control approaches are discussed in Section 2 and Section 3. The individual contributions of the paper are as follows: we demonstrate how to identify a suitable Neural Network (NN) to capture the dynamics of building envelope and HVAC control system. We investigate several choices of lags for states, controls, and disturbances and provide insight into best practices. We also present different MPC formulations, assisted by using AD, to maintain occupants' comfort constraints while minimizing KPIs for HVAC energy consumption. We show the customizability of the framework through the ease of using two different control approaches to solve the MPC problem. We show that the proposed approach can be used to warm-start the receding horizon replanning for the MPC problem. In the result section, we also provide a performance comparison between different approaches for modeling and solving NMPC when operating on computationally intensive hybrid system models. We also discuss potential best practices based on desired control criteria (speed, optimality, etc.). Finally, to the best of our knowledge, the NMPC control of the BOPTEST five-zone model is the first of its kind. We believe this framework is scalable for data-driven NMPC control of the BOPTEST, and potentially other physics-based building emulators, that are being developed for prototyping controllers in large building HVAC systems.

# 2. SURROGATE MODELING FOR BUILDING EMULATOR

Our aim is to replace the computationally expensive nonlinear numerical simulations with alternative, fast representations for model-based control. In the context of using NNs for MPC, we believe that one should include the following criteria in their surrogate modeling process:

- Computing cost: Small computing cost for fast iterative evaluations.
- Predictive accuracy: Good prediction accuracy for MPC's horizon.
- Differentiability: Fast and accurate gradient information for successive linearization, nonlinear solvers, etc., for different MPC formulations.

We leverage Pytorch (Paszke et al., 2019) modeling library to meet these goals. In this study, we consider the following cases: Linear, MLP, and Long short-term memory (LSTM). MLP has a fast forward computation and good expressivity to approximate complex functions Hornik et al. (1989). On the other, since BOPTEST is Partially Observable MDP (POMDP), it requires lag information from states, actions, and time-varying disturbance for model fitting. This can be curtailed by using LSTM which has proven to work well for nonlinear mappings with autoregressive features Siami-Namini et al. (2018). While fairly simple, the linear model has the advantage of fastest model evaluations and plug-and-play viability for fast QP solvers.

#### 2.1 Linear

The surrogate model takes its input as the states x, control inputs u, time-varying disturbances d, and their lags of past time-steps. The output of the surrogate model is the future state prediction  $\{x_{t+1}\}$ , i.e.,:

$$x_{t+1} = f(x_{t-M_x:t}, u_{t-M_u:t}, d_{t-M_d:t})$$
 (2)

where  $M_x, M_u, M_d$  are state, input and disturbance lags, respectively. Since the choices of lags are application dependent, we discuss this further in the result section. Here, f is linearized as follows:

$$x_{t+1} = \sum_{k=0}^{M_x} A_k x_{t-k} + \sum_{k=0}^{M_u} B_k u_{t-k} + \sum_{k=0}^{M_d} C_k d_{t-k}$$
 (3)

where  $A_k = \nabla_x f \in \mathbb{R}^{N_x \times N_x}$ ,  $B_k = \nabla_u f \in \mathbb{R}^{N_x \times N_u}$  and  $C_k = \nabla_d f \in \mathbb{R}^{N_x \times N_d}$  are learnable parameter matrices for state, control input and disturbance, respectively.

#### 2.2 MLP

The linearized model given by Equation 3 also applies here. The forward computation in MLP is written as the following:

$$h_0 = [x_{t-M_x}, u_{t-M_u}, d_{t-M_d}]$$

$$h_{k+1} = \tanh(W_k h_k + b_k), \qquad k = \{0, ..., K-1\}$$

$$x_{t+1} = o_{t+1} = W_K h_K + b_K$$
(4)

where  $h_k \in \mathbb{R}^l$  is a hidden unit of the layer k,  $W_k$  and  $b_k$  are weight parameters of the layer k.

#### 2.3 LSTM

The forward computation of LSTM is written as the following:

$$h_{t}, c_{t} = MLP_{\text{enc}}(x_{t-M_{x}:t}, u_{t-M_{u}:t-1}, d_{t-M_{u}:t})$$

$$i_{t} = \sigma(W_{ii}u_{t} + b_{ii} + W_{hi}h_{t-1} + b_{hi})$$

$$f_{t} = \sigma(W_{if}u_{t} + b_{if} + Ww_{hf}h_{t-1} + b_{hf})$$

$$g_{t} = tanh(W_{ig}u_{t} + big + W_{hg}h_{t} + b_{hg})$$

$$o_{t+1} = \sigma(W_{io}u_{t} + b_{io} + W_{ho}h_{t} + b_{ho})$$

$$c_{t+1} = f_{t} \odot c_{t} + i_{t} \odot g_{t}$$

$$h_{t+1} = o_{t} \odot tanh(c_{t+1})$$

$$x_{t+1} = MLP_{\text{dec}}(h_{t+1})$$
(5)

where  $h_t$  is the hidden state,  $c_t$  is the cell state,  $i_t$ ,  $f_t$ ,  $g_t$  and  $o_t$  are the input, forget, cell, and output gates, respectively.  $\sigma(\cdot)$  is the sigmoid function,  $\odot$  is the Hadamard product, and  $MLP_{\rm enc}$  and  $MLP_{\rm dec}$  are a MLP encoder and decoder, respectively.

#### 3. CONTROL PROBLEM FORMULATION

Consider the discrete-time nonlinear dynamical system:

$$x_{t+1} = f(x_t, u_t, d_t),$$
 (6)

where  $x_t \in \mathbb{R}^{n_x}$  and  $u_t \in \mathbb{R}^{n_u}$  correspond to the state and control vectors at time t and  $d_t \in \mathbb{R}^{n_d}$  is the set of contextual variables/external inputs. The optimal control problem is to find the optimal control policy that minimizes the cumulative cost:

$$\min_{u_t} \sum_{t=0}^{T} c_t(x_t, u_t, d_t)$$
Subject to:  $x_{t+1} = f(x_t, u_t, d_t)$ , (8)

Subject to: 
$$x_{t+1} = f(x_t, u_t, d_t),$$
 (8)

Subject to: 
$$u_t^l \le u_t \le u_t^u$$
, (9)

for given  $x_0$ , and where  $c_t(\cdot)$  is the instantaneous cost function given as:

$$c_t(\cdot) = P_c + P_h + L_k + \gamma P_x,\tag{10}$$

where  $P_c$  and  $P_h$  are total cooling and heating cost,  $L_k = \|\tilde{u}_{t+1} - \tilde{u}_t\|_R^2$  is a regularizer term, which penalizes large changes in the control inputs to avoid undesirable oscillations, and  $P_x = \max(x_t^l - x_t, 0) + \max(x_t - x_t^u, 0)$ enforces the occupant comfort constraints implemented with ReLU function with a penalty coefficient  $\gamma$ . The problem also considers input box constraints with lower and upper bound given as  $[u_t^l, u_t^u]$ .

#### 3.1 Gradient Descent Method

The gradient descent method is one of the widely-used algorithms to optimize a differentiable objective function. At each iteration, the gradient of the objective function is computed and the decision variables are updated in direction of the computed gradient. Gradient descent algorithms have a precedent across domains such as training neural networks Schmidhuber (2015) and solving optimal control problems (Lin et al., 2014). In this paper, we use Adam (Kingma and Ba, 2014), which has shown promising results in deep learning applications. For input constraint (9), we use projected gradient descent, a common method in solving constrained optimization: after each gradient update, we project the control vector  $u_t$  into a feasible region  $[u_t^l, u_t^u]$ . Since the feasible region is a box constraint, the projected control vector is easily computed by using a clamp function after each update of the algorithm.

#### 3.2 Sequential Quadratic Programming

There have been numerous tools and methods developed to solve specific nonlinear optimization problems with particular structures of cost functions, equality, and inequality constraint functions. However, Sequential Quadratic Programming (SQP) remains one of the most efficient approaches to solving any general constrained-nonlinear optimization problem. For the SQP approach, we utilize the optimization subroutine originally proposed by Dieter Kraft Kraft (1988) and as implemented in SciPy Virtanen et al. (2020) to solve the control optimization problem described in Eqns. (7-9). The algorithm is a quasi-Newton method (using BFGS) applied to a Lagrange function consisting of a loss function and equality and inequality constraints. In our implementation, we provide the function evaluations, which are calculated using Equation 10, and it's Jacobian using automatic differentiation. Instead of clamping, we pass bounds for control inputs directly to the solver.

#### 4. RESULTS

We demonstrate the effectiveness of our control framework for controlling building models in BOPTEST (Blum et al., 2021), a software for simulation-based benchmarking of building HVAC control algorithms. The rest of this section details two test cases that demonstrate the results of deriving different surrogate models and discusses the subsequent control results for the control algorithms described in Section 3.

#### 4.1 Model Description

BOPTEST emulators use Modelica (Wetter et al., 2014) to represent realistic physical dynamics. Embedded in these models are baseline control algorithms that can be overwritten using supervisory and local-loop control signals. BOPTEST uses a containerized run-time environment (RTE) which enables rapid, repeatable deployment of models. Using this feature, we stand up several instances of models on servers and query these models to speed-up data generation at scale for surrogate modeling. We also test controls on the same containers, representing digitaltwins of real buildings. We consider the following case studies:

BESTEST Case 900 model This test case is a single room with floor dimensions of 6m x 8m and a floor-toceiling height of 2.7m. The building is assumed to be occupied by two people from 8 am to 6 pm each day. Heating and cooling are provided to the office using an idealized four-pipe fan coil unit (FCU), presented in Figure 1. The FCU contains a fan, cooling coil, and heating coil. The fan draws room air into the HVAC unit and supplies the conditioned air back to the room. No outside air is mixed during this process. The fan has a variable speed drive serving the fan motor. The cooling coil is served by chilled water produced by a chiller and the heating coil is served by hot water produced by a gas boiler. Two different PI controllers for heating and cooling modulate the supply air temperature and fan speed to provide cooling and heating load to the room. The schematics and control

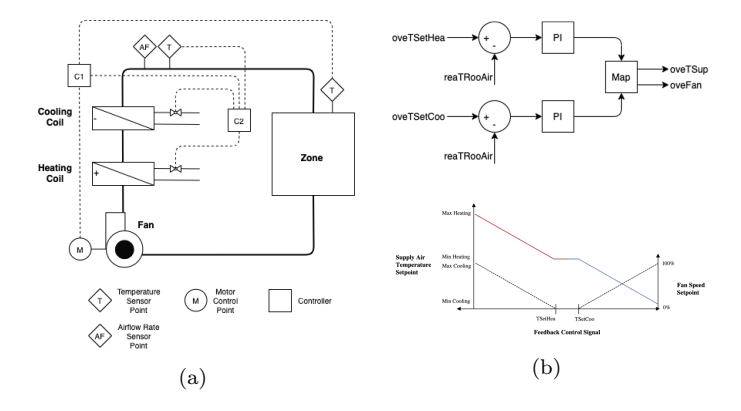


Fig. 1. Control schematics of the BESTEST Case 900 model. Source: https://ibpsa.github.io/project1-boptest/

mapping are shown in Figure 1. For our supervisory MPC controller, we manipulate supply air temperature and fan speed as control inputs to minimize the combined cooling, heating, and fan power consumption while maintaining the occupant comfort bounds. Assuming the building to be in a climate close to Denver, CO, USA, the state and input box constraints are as follows:

$$21^{o}C \le x^{T_{zone},occ} \le 24^{o}C \tag{11}$$

$$15^{o}C \le x^{T_{zone},unocc} \le 30^{o}C \tag{12}$$

$$0.0 \le u^{fan} \le 1.0 \tag{13}$$

$$12^{o}C < u^{T_{supp}} < 40^{o}C \tag{14}$$

Multi-zone office (ASHRAE 2006 VAVReaheat) The test case represents the middle floor of an office building located in Chicago, IL, as described in the set of DOE Commercial Building Benchmarks for new construction (Deru et al., 2011) with weather data from TMY3 for Chicago O'Hare International Airport. The represented floor has five zones, with four perimeter zones and one core zone. The occupied time for the HVAC system is between 6 AM and 7 PM each day. The HVAC system is a multi-zone single-duct Variable Air Volume (VAV) system with pressure-independent terminal boxes with reheat. A schematic of the system is shown in Figure 2. The cooling and heating coils are water-based, served by an air-cooled chiller and air-to-water heat pump respectively. A number of low-level, local-loop controllers are used to maintain the desired setpoints using the available actuators. The primary local-loop controllers are specified on the diagrams of Figure 3 as C1 to C3. C1 is responsible for maintaining the zone temperature setpoints as determined by the operating mode of the system and implements dual-maximum logic. C2 is responsible for maintaining the duct static pressure setpoint and implements a duct static pressure reset strategy. C3 is responsible for maintaining the supply air temperature setpoint as well as the minimum outside air flow rate as determined by the operating mode of the system. In this case, we assume the fan speed to be constant and our supervisory MPC controller manipulates the damper position and reheat control signal to control the airflow and zone supply air temperature respectively (at each zone). In addition, the central HVAC cooling and

heating units are manipulated to control the central supply air temperature. The optimization objective is to minimize the overall cooling and heating loads while maintaining the occupant comfort bounds and central supply air temperature. The state and input box constraints are as follows:

$$21^{\circ}C \le x^{T_{zone_i},occ} \le 24^{\circ}C \tag{15}$$

$$15^{o}C \le x^{T_{zone_i},unocc} \le 30^{o}C \tag{16}$$

$$0.0 \le u^{dam_i} \le 1.0$$
 (17)

$$0.0 < u^{yReaHea_i} < 1.0 \tag{18}$$

 $\forall i \in \{1, 2, 3, 4, 5\}$ 

$$5^{\circ}C \le x^{T_{supp}} \le 20^{\circ}C \tag{19}$$

$$0.0 \le u^{yHea} \le 1.0$$
 (20)

$$0.0 \le u^{yCoo} \le 1.0 \tag{21}$$

#### 4.2 System Identification

We consider the three choices of models as described in Section 2 for the single zone and multi-zone case. We describe how we sufficiently excite the system to generate data and report the training and out-of-training performance of each model.

Data generation For each time-step t=0,...,T-1, we sample a random control input  $u_t$  from a uniform distribution of the feasible input space and pass the sampled control input to BOPTEST simulation to get the next observation and disturbance. We collect the data up to time-step T, and repeat this procedure K times using different initial conditions. In the BESTEST case, we choose  $K=120,\,T=500,$  and use 100 distinct trajectories as training data, 10 for validation and 10 for test. In the

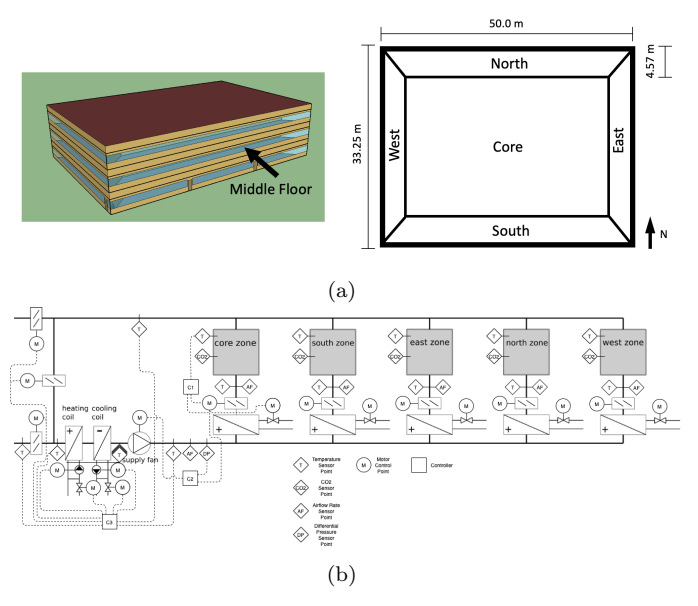


Fig. 2. Envelope, Floorplan and control schematics of multi zone office air simple emulator model of BOPTEST. Source: https://ibpsa.github.io/project1-boptest/

Table 1.
$MSE (\times 10^{-5})$
for
dif-
fer-
ent
model
choices
in
BESTEST
case

Model	Train MSE	Val MSE	Test MSE
Linear	699.5	566.8	780.3
MLP	8.846	12.70	17.56
LSTM	1.418	1.726	2.145

multi-zone office case, we choose  $K=600,\,T=1000,\,$  and use 500 trajectories as the training dataset, and keep 50 for validation and 50 for test purposes. It is evident that test data, which all results are reported on, is the data that the model has never been trained on.

Hyperparameters The MLP framework consists of 4 layers with 256 nodes in each layer, and  $\tanh(\cdot)$  activation layers in-between the MLP layers. For the LSTM model, we implement 2 layers with 256 nodes for  $MLP_{\rm enc}$  and  $MLP_{\rm dec}$  and choose the dimension of hidden and cell state as 256. Mean squared error (MSE) is used for computing training loss. For all surrogate models, we choose Adam to optimize the parameters with learning rate=0.001, and epoch=1000.

Predictive performance Table 1 and Table 2 show the results of test performance for single-zone and five-zone

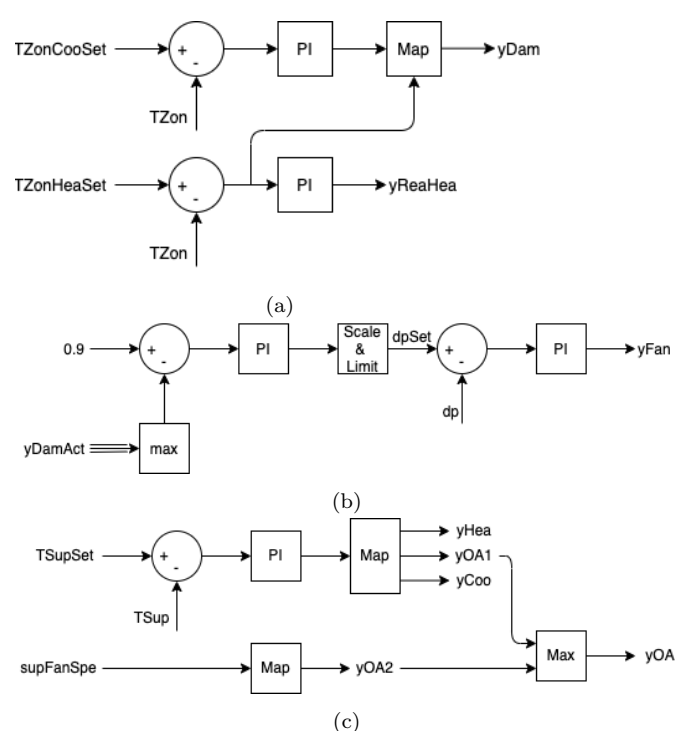


Fig. 3. Lower-level control schematics for five-zone model. Source: https://ibpsa.github.io/project1-boptest/

Table $2$ .
$MSE (\times 10^{-5})$
for
dif-
fer-
ent
MLP
hy-
per-
pa-
ram-
e-
ter
choices
in
multi-
zone
of-
fice
case

$(M_x, M_u, M_d)$	Train MSE	Val MSE	Test MSE
(1, 1, 1)	511.6	623.9	618.6
(1, 1, 5)	476.0	623.8	624.3
(1, 5, 1)	20.46	21.74	24.35
(5, 1, 1)	82.43	98.92	103.8
(1,5,5)	14.71	17.76	18.47
(5, 1, 5)	78.38	98.17	100.06
(5, 5, 1)	21.20	23.67	26.87
(5, 5, 5)	10.37	14.80	14.82

models respectively. Losses are calculated using average prediction error for 40 steps. For multi-step ahead prediction, a for-loop is implemented in the forward propagation of the ML models. The results for single-zone and multi-zone models demonstrate the superiority of LSTM in prediction accuracy, although, MLP performance is comparable in the five-zone case as depicted in Figure 4.

In Table 2, we compare the performance of different MLP model choices with different lag values of the state, input, and time-varying disturbances. (5,5,5) is the best model among all choices but (1,5,5) model comes very close with fewer model inputs. This model depends on lags of weather data and control inputs, which we speculate is not unrelated to the lags associated with lower-level controllers in this system. We chose (1,5,5) as a more simple, equally accurate choice. Figure 5 is a visual depiction of the predictive accuracy of the chosen MLP for surrogate modeling of the five-zone model during three distinct weather events (January, May, and August) for the core zone. Each orange trajectory is a 50-step ahead prediction (12.5 hours) starting from the leftmost point of the trajectory. These results appear to be conclusive for deploying the model in MPC.

#### 4.3 Control Results

For all control algorithms, we deploy a receding-horizon controller, wherein a 10-step "look-ahead" trajectory is generated using the optimization algorithm, and only the first step of the optimization solution is passed to BOPTEST model to obtain new measurements. The new data point is then used as the initial condition for the next iteration of the control optimization. In addition, to

speed up convergence, the previously optimized control trajectory is used as the initial trajectory for warm-starting the receding horizon replanning for the MPC problem.

The control results for single-zone and multi-zone cases are reported in Table 3 and Table 4, respectively. In the single-zone case, LSTM model performs best for control. This is expected from the superior predictive accuracy of the model. flt also has the best average computation time. As or the control algorithm, Gradient-based approach finds a better local minima for the problem. In the multi-zone case, LSTM performs poorly (unexpectedly) and MLP outperforms all models. Here, in contrast to the previous case, SLSQP finds a better local minima. Next, we discuss the significance of these results.

#### 4.4 Discussion

The modeling results indicate that it is possible to derive accurate ML models from the building emulators. It is worth mentioning that the bottleneck in this process is data generation which is not always trivial for hybrid systems with many if-else conditions, low-level control loops and system constraints, and finely-tuned numerical solvers.

On the control side, we have run extensive tests using SLSQP and Gradient-based approaches from different initial conditions. In the one-zone case, the gradient-based approach with the LSTM model shows the lowest power consumption with an acceptable discomfort level. However, in the multi-zone case, SLSQP with MLP model reaches the lowest power consumption, even though LSTM model shows better predictive performance. This can happen when the optimization problem in the control formulation is highly non-convex. The complexity of the surrogate model likely creates many additional local minima, which in turn, depreciates the control performance. This, somewhat contradictory, implies that better predictive performance does not always guarantee better control performance. We believe that based on this experiment, a middle-ground between model complexity and predictive performance should be considered for these types of MPC problems. Alternatively, better control formulations might help to curb this issue. Since we have found little precedent in the literature, we are running more tests to find better

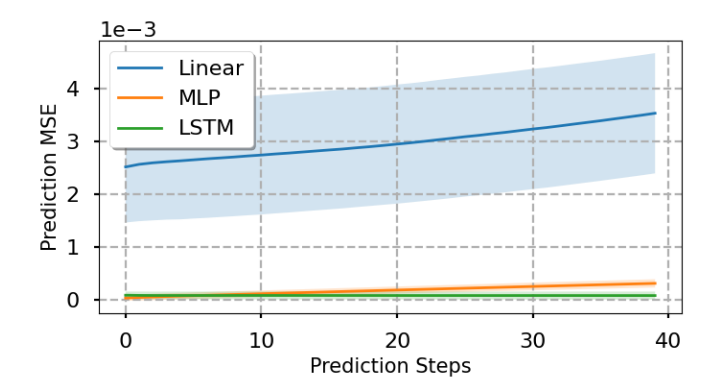


Fig. 4. Test MSE for different choices of surrogate models in multi-zone test case. LSTM and MLP have comparable performance and outperform the Linear model.

Table 3. Average of total  $power(kWh/m^2),$ thermal discomfort (kh/zone)and computation time (sec)on BESTEST case

Model	Solver	Power	Discomfort	Time
Linear	GDM	0.0189	1556	1.607
Linear	SLSQP	0.2551	1528	0.933
MLP	GDM	4.804	2.935	1.694
MLP	SLSQP	5.059	5.207	1.684
LSTM	GDM	4.818	2.081	0.620
LSTM	SLSQP	4.943	4.415	0.661

and more definitive answers. It is also worth pointing out that the framework is working as designed, helping to frame new hypotheses based on experimentation.

By comparing the average compu-Computation Time tation time between several methods, we make the following interesting observations: First, both the gradientbased approach and SLSQP show comparable computation time, though the computation time of both solvers depends on their stopping criteria. For example, after running extensive tests, we decided that 100 iterations was a good stopping criteria for the gradient-based approach. We expect this hyperparameter tuning to be problem specific. Second, for the surrogate model, it is obvious to us that MLP should take longer than the Linear model to run. Surprisingly, the LSTM model, which has the most complex structure among the three candidates, shows the fastest computation time. We think that this computation time gap most likely comes from a difference in the implementation language. Each surrogate model has a for-loop to predict the multi-steps. Although all surrogate models are implemented in Pytorch, the linear and MLP model conduct their for-loops in python, while LSTM model uses C++.

#### 5. CONCLUSION AND FUTURE WORK

We presented a modeling and control framework for controlling physics-based building emulators. We have shown that our approach is successful in reducing cooling and heating loads in the BOPTEST emulator while satisfying

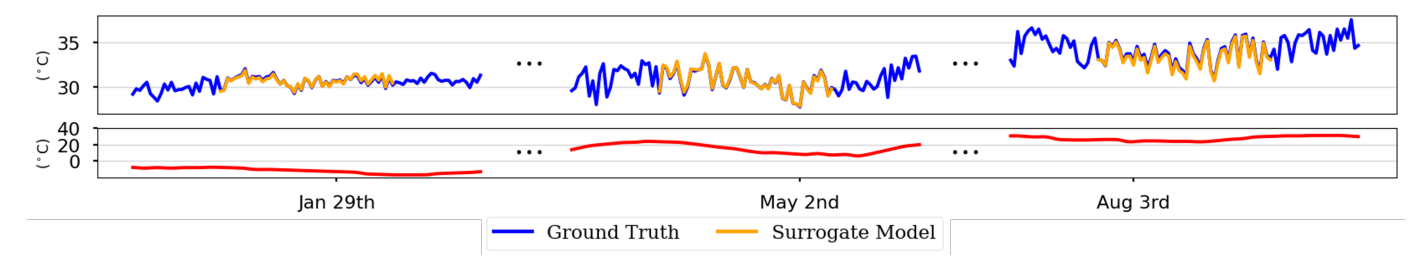


Fig. 5. The set of figures show the results of out-of-training predictive performance for five zone model during three distinct weather events (January, May, and August) for core zone (top). The ambient temperature trajectories is depicted in red (bottom). The orange lines represent the 50-step ahead predictions (12.5 hours) starting from the left most point of the trajectory. The full MSEs are reported in Table 2.

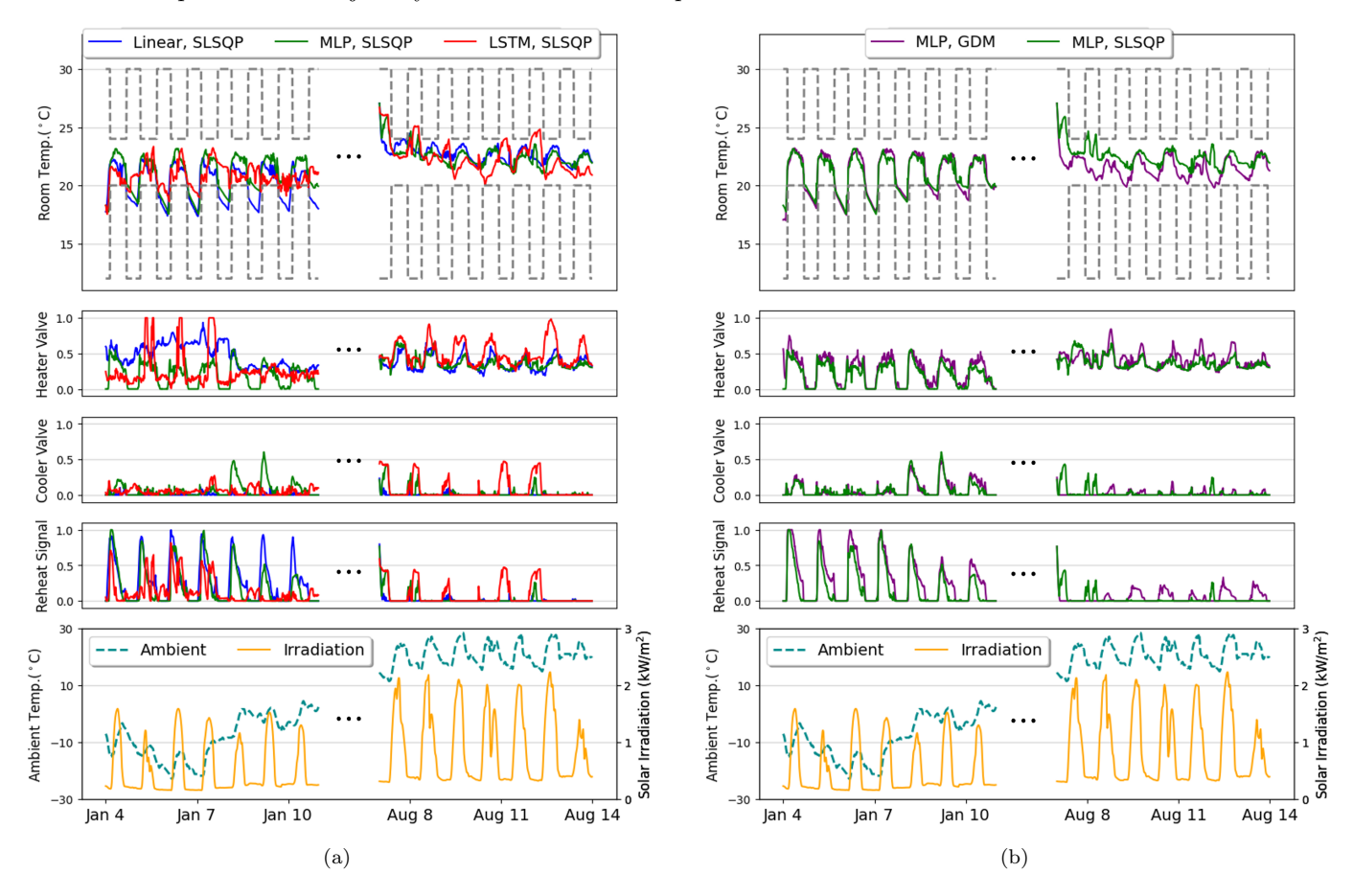


Fig. 6. Result comparison for different choices of models and control algorithms. The top figure represents the temperate. The bottom figure is the relevant weather data, and the middle figures are the corresponding control inputs. The results are divided into a cold (Jan) and hot (Aug) weather events. (a) Result for control of core-zone in the multi-zone test case using SLSQP with Linear, MLP, and LSTM models. Using MLP model, the control outperforms LSTM and Linear model-based implementation. (b) MLP-based control results with SLSQP solver slightly outperform the Gradient-based approach.

occupant comfort and adhering to control system constraints. The approach is modular, meaning that it will be compatible with various other choices of models and control algorithms. For example, while we did not succeed in training a good LSTM model for the five-zone case, we anticipate that the right hyperparameter tuning should address this issue and we are actively working on it. The same is true for control. For example, we tested the framework with an iLQR controller which failed to satisfy constraints. While we did not manage to get the results

we expected, we anticipate that significantly better control results are possible with iLQR and we are currently fixing our implementation of the algorithm. This is especially important since iLQR has shown superior performance for nonlinear optimal control problems (Li and Todorov, 2007). We are also exploring other fast first-order solvers with alternative control formulations. For example, we are considering OSQP (Stellato et al., 2020), which will significantly speed up the optimization while producing high-quality solutions, or distributed ADMM (Boyd et al.,

Table 4. Average of total  $power(kWh/m^2),$ thermal discomfort (kh/zone)and computation time (sec)on multizone office case

Model	Solver	Power	Discomfort	Time
Linear	GDM	2.807	10.44	1.504
Linear	SLSQP	2.487	11.40	1.600
MLP	GDM	3.458	4.054	1.782
MLP	SLSQP	2.778	3.154	2.144
LSTM	GDM	2.222	124.7	0.570
LSTM	SLSQP	2.880	35.48	0.818

2011) for district-level problems. In addition, We are actively working with the developers of BOPTEST to control scaled-up models, including multiple coupled buildings, with the framework.

The main bottleneck for scaling the current approach is the customized nature of the data generation process. In the current process, many trials and errors are required to find a feasible input space that does not break the emulator in forward simulations. Latest studies(Chakrabarty et al., 2022) provide some promising insight into more robust sampling procedures. We are currently working on incorporating similar approaches into our process.

Last but not least, while in this paper we focused on control as an application, we firmly believe that system design, fault diagnosis, and reliability are other applications that will benefit from the proposed modeling approach, and we are actively investigating problems in these domains.

### REFERENCES

- Atam, E. and Helsen, L. (2016). Control-oriented thermal modeling of multizone buildings: Methods and issues: Intelligent control of a building system. *IEEE Control systems magazine*, 36(3), 86–111.
- Blum, D., Arroyo, J., Huang, S., Drgoňa, J., Jorissen, F., Walnum, H.T., Chen, Y., Benne, K., Vrabie, D., Wetter, M., et al. (2021). Building optimization testing

- framework (boptest) for simulation-based benchmarking of control strategies in buildings. *Journal of Building Performance Simulation*, 14(5), 586–610.
- Boyd, S., Parikh, N., Chu, E., Peleato, B., Eckstein, J., et al. (2011). Distributed optimization and statistical learning via the alternating direction method of multipliers. Foundations and Trends® in Machine learning, 3(1), 1–122.
- Chakrabarty, A., Bortoff, S.A., and Laughman, C.R. (2022). Simulation failure-robust bayesian optimization for data-driven parameter estimation. *IEEE Transactions on Systems, Man, and Cybernetics: Systems.*
- Deru, M., Field, K., Studer, D., Benne, K., Griffith, B., Torcellini, P., Liu, B., Halverson, M., Winiarski, D., Rosenberg, M., et al. (2011). Us department of energy commercial reference building models of the national building stock. *National Renewable Energy Laboratory*.
- Drgoňa, J., Arroyo, J., Figueroa, I.C., Blum, D., Arendt, K., Kim, D., Ollé, E.P., Oravec, J., Wetter, M., Vrabie, D.L., et al. (2020). All you need to know about model predictive control for buildings. Annual Reviews in Control.
- Henderson, P., Islam, R., Bachman, P., Pineau, J., Precup, D., and Meger, D. (2018). Deep reinforcement learning that matters. In *Thirty-Second AAAI Conference on Artificial Intelligence*.
- Hornik, K., Stinchcombe, M., and White, H. (1989). Multilayer feedforward networks are universal approximators. *Neural networks*, 2(5), 359–366.
- Kingma, D.P. and Ba, J. (2014). Adam: A method for stochastic optimization. arXiv preprint arXiv:1412.6980.
- Kraft, D. (1988). A software package for sequential quadratic programming. Forschungsbericht- Deutsche Forschungs- und Versuchsanstalt fur Luft- und Raumfahrt.
- Levine, S., Finn, C., Darrell, T., and Abbeel, P. (2016). End-to-end training of deep visuomotor policies. The Journal of Machine Learning Research, 17(1), 1334– 1373.
- Li, W. and Todorov, E. (2007). Iterative linearization methods for approximately optimal control and estimation of non-linear stochastic system. *International Journal of Control*, 80(9), 1439–1453.
- Lillicrap, T.P., Hunt, J.J., Pritzel, A., Heess, N., Erez, T., Tassa, Y., Silver, D., and Wierstra, D. (2015). Continuous control with deep reinforcement learning. arXiv preprint arXiv:1509.02971.
- Lin, Q., Loxton, R., and Teo, K.L. (2014). The control parameterization method for nonlinear optimal control: a survey. *Journal of Industrial and management optimization*, 10(1), 275–309.
- Mostafavi, S., Doddi, H., Kalyanam, K., and Schwartz, D. (2022). Nonlinear moving horizon estimation and model predictive control for buildings with unknown hvac dynamics. *Ifac-Papersonline*, Accepted.
- Oei, M., Guenther, J., Böhm, M., Park, S., and Sawodny, O. (2020). A bilinear approach to model predictive control for thermal conditioning of adaptive buildings. IFAC-PapersOnLine, 53(2), 8383–8388.
- O'Dwyer, E., Atam, E., Falugi, P., Kerrigan, E., Zagorowska, M., and Shah, N. (2022). A modelling workflow for predictive control in residential buildings.

- In Active Building Energy Systems, 99–128. Springer.
- Paszke, A., Gross, S., Chintala, S., Chanan, G., Yang, E., DeVito, Z., Lin, Z., Desmaison, A., Antiga, L., and Lerer, A. (2017). Automatic differentiation in pytorch. 31st Conference on Neural Information Processing Systems (NIPS 2017), Long Beach, CA, USA.
- Paszke, A., Gross, S., Massa, F., Lerer, A., Bradbury, J.,
  Chanan, G., Killeen, T., Lin, Z., Gimelshein, N., Antiga,
  L., et al. (2019). Pytorch: An imperative style, high-performance deep learning library. Advances in neural information processing systems, 32.
- Schmidhuber, J. (2015). Deep learning in neural networks: An overview. *Neural networks*, 61, 85–117.
- Siami-Namini, S., Tavakoli, N., and Namin, A.S. (2018). A comparison of arima and lstm in forecasting time series. In 2018 17th IEEE international conference on machine learning and applications (ICMLA), 1394–1401. IEEE.
- Silver, D., Huang, A., Maddison, C.J., Guez, A., Sifre, L.,
  Van Den Driessche, G., Schrittwieser, J., Antonoglou,
  I., Panneershelvam, V., Lanctot, M., et al. (2016).
  Mastering the game of go with deep neural networks and tree search. nature, 529(7587), 484.
- Stellato, B., Banjac, G., Goulart, P., Bemporad, A., and Boyd, S. (2020). Osqp: An operator splitting solver for quadratic programs. *Mathematical Programming Computation*, 12(4), 637–672.
- Sturzenegger, D., Gyalistras, D., Morari, M., and Smith, R.S. (2015). Model predictive climate control of a swiss office building: Implementation, results, and costbenefit analysis. *IEEE Transactions on Control Systems Technology*, 24(1), 1–12.
- Todorov, E. and Li, W. (2005). A generalized iterative LQG method for locally-optimal feedback control of constrained nonlinear stochastic systems. In *Proceedings* of American Control Conference, 300 306.
- United States Energy Information Administration (2021). Total energy monthly data. URL https://www.eia.gov/totalenergy/data/monthly/.
- Virtanen, P., Gommers, R., Oliphant, T.E., Haberland, M., Reddy, T., Cournapeau, D., Burovski, E., Peterson, P., Weckesser, W., Bright, J., et al. (2020). Scipy 1.0: fundamental algorithms for scientific computing in python. *Nature methods*, 17(3), 261–272.
- Walker, S.S., Lombardi, W., Lesecq, S., and Roshany-Yamchi, S. (2017). Application of distributed model predictive approaches to temperature and co2 concentration control in buildings. *IFAC-PapersOnLine*, 50(1), 2589–2594.
- Wetter, M., Zuo, W., Nouidui, T.S., and Pang, X. (2014). Modelica buildings library. *Journal of Building Performance Simulation*, 7(4), 253–270.